Flagellum and toxin phase variation impacts intestinal colonization and disease development in a mouse model of *Clostridioides difficile* infection

Dominika Trzilova, Mercedes A. H. Warren, Nicole C. Gadda, Caitlin L. Williams, and Rita Tamayo*

Department of Microbiology and Immunology, University of North Carolina at Chapel Hill School of Medicine, Chapel Hill, NC, USA

*Corresponding Author
125 Mason Farm Rd, CB #7290
Chapel Hill, NC 27599-7290
Email: rita_tamayo@med.unc.edu
(919) 843-2864

KEYWORDS: phenotypic heterogeneity, motility, flagella, toxin, mouse, hamster

Abstract

Clostridioides difficile is a major nosocomial pathogen that can cause severe, toxin-mediated diarrhea and pseudomembranous colitis. Recent work has shown that *C. difficile* exhibits heterogeneity in swimming motility and toxin production *in vitro* through phase variation by site-specific DNA recombination. The recombinase RecV reversibly inverts the flagellar switch sequence upstream of the *flgB* operon, leading to the ON/OFF expression of flagellum and toxin genes. How this phenomenon impacts *C. difficile* virulence *in vivo* remains unknown. We identified mutations in the right inverted repeat that reduced or prevented flagellar switch inversion by RecV. We introduced these mutations into *C. difficile* R20291 to create strains with the flagellar switch "locked" in either the ON or OFF orientation. These mutants exhibited a loss of flagellum and toxin phase variation during growth *in vitro,* yielding precisely modified mutants suitable for assessing virulence *in vivo*. In a hamster model of acute *C. difficile* infection, the phase-locked ON mutant caused greater toxin accumulation than the phase locked OFF mutant but did not differ significantly in the ability to cause acute disease symptoms. In contrast, in a mouse model, preventing flagellum and toxin phase variation affected the ability of *C. difficile* to colonize the intestinal tract and to elicit weight loss, which is attributable to differences in toxin production during infection. These results show that the ability of *C. difficile* to phase vary flagella and toxins influences colonization and disease development and suggest that the phenotypic variants generated by flagellar switch inversion have distinct capacities for causing disease.

Introduction

Many bacterial species employ phase variation to generate phenotypic heterogeneity within a clonal population. Bacteria frequently encounter selective pressures in their environment, and phenotypic heterogeneity helps ensure survival by creating subpopulations that are differentially equipped to overcome these pressures.[1] Phase variation typically affects the production of surface factors that directly interface with the bacterium's environment, such as flagella, pili, and exopolysaccharides. Both mucosal pathogens and commensal species employ phase variation to balance the fitness advantages conferred by these structures with the costs of producing them; in a host environment, the ability to phase vary can promote immune evasion and persistence in the host.[2] Phase variation can be achieved by multiple epigenetic and genetic mechanisms, including DNA modification by methylation, slipped-strand mispairing, homologous recombination, and site-specific recombination.[1, 3]

In many pathogens including *Acinetobacter baumannii*, *Bordetella bronchiseptica*, and *Streptococcus pneumoniae,* host selective pressures can substantially affect the composition of a phase-variable bacterial population during infection.[4-11] All three of these pathogens can form distinct subpopulations differentially equipped for survival in disparate environments. However, determining the importance of phase variation (rather than the phase-variable trait) in pathogenesis can be challenging. Studies in which phase variation has been eliminated to create "phase-locked" mutants have been valuable for determining the impact of phase variation itself. In *B. bronchiseptica*, phase-locked Bvg+ and Bvg- strains were created by either deleting *bvgS* encoding the sensor kinase in the BvgAS system (Bvg- phase) or mutating BvgS to be constitutively active (Bvg+ phase).[4] Phase-locked strains have also been created by mutating site-specific recombinases that mediate inversion of one or multiple loci, e.g., Mpi modulating

polysaccharide production in *Bacteroides fragilis*.[12] Finally, in uropathogenic *Escherichia coli* (UPEC), mutation of inverted repeats critical for site-specific recombination generated populations unable to phase vary the production of fimbriae.[13, 14] These studies led to improved understanding of host-microbe interactions and the importance of phase variation in fitness of bacterial pathogens in diverse host environments.

Clostridioides difficile is a gram-positive, spore-forming anaerobe that is currently the leading cause of antibiotic-associated diarrheal disease and one of the most common causes of nosocomial infection. *C. difficile* infection (CDI) is primarily mediated by two toxins, TcdA and TcdB, that glucosylate and inactivate Rho family GTPases leading to perturbation of the actin cytoskeleton.[15-17] During infection, TcdA and TcdB disrupt the intestinal epithelial barrier resulting in inflammation, immune cell recruitment, and development of diarrheal symptoms,[18] and evidence suggests both toxins are important for disease development in animal models.[19-21]

Several recent studies have shown that *C. difficile* exhibits substantial phenotypic heterogeneity via phase variation by site-specific DNA recombination.[22-26] This mechanism of phase variation is mediated by serine or tyrosine DNA recombinases that recognize sequences containing inverted repeats and catalyze strand exchange, leading to inversion of the intervening DNA sequence.[27, 28] Eight DNA sequences that can undergo inversion have been identified in *C. difficile*, though individual strains may contain only a subset.[24, 29] Three of these sequences have been experimentally demonstrated to modulate expression of adjacent genes leading to phase variation of the encoded factors: the cell wall protein CwpV,[22, 30] flagella,[23, 31] and the CmrRST signal transduction system.[26]

C. difficile flagella are required for swimming motility and contribute to adherence to intestinal epithelial cells, colonization, and virulence in animal models of infection.[32-35] Flagellar

genes in *C. difficile* are organized in multiple operons that are expressed in a hierarchical manner coordinated by the sigma factor SigD (also known as FliA and σ^{28}).[36-39] SigD also promotes expression of toxin genes by activating transcription of *tcdR*, which encodes a direct positive regulator of *tcdA* and *tcdB*, linking toxin production to flagellar gene transcription.[38-40] Consistent with these findings, phase variation of flagella results in concomitant phase variation of toxin biosynthesis *in vitro*.[23, 25, 41] This phase variation occurs as a result of inversion of a DNA sequence, termed the flagellar (*flg*) switch, upstream of the *flgB* coding sequence and mapping to the 5' untranslated region of the *flgB* operon.[23] The flagellar switch is flanked by imperfect inverted repeats and contains regulatory features that control gene expression by a mechanism dependent on Rho-mediated transcription termination.[41] This process generates a phenotypically heterogeneous population consisting of *flg* ON cells that are motile and toxigenic and *flg* OFF cells that are aflagellate, nonmotile, and attenuated for toxin production.[23, 41]

The roles of flagella and toxins in *C. difficile* pathogenesis are well studied, but the importance of the heterogeneity generated by their phase variation to disease development is unknown. The goal of this study was to analyze the effects of preventing phase variation of the flagellar switch on *C. difficile* physiology and virulence. Phase-locked 'ON' and 'OFF' mutants were previously generated by eliminating the site-specific tyrosine recombinase, RecV, and identifying isolates with the flagellar switch locked in either orientation.[22] However, RecV is required for inversion of three other sequences (upstream of *cwpV*, *cmrRST*, and CDR20291_0963) and influences inversion of two additional sequences (upstream of CDR20291_0685 and CDR20291_1514).[22-24, 26, 42] The broad regulation exerted by RecV thus results in pleiotropic effects that limit the utility of *recV* mutants for studying the impact of flagellum and toxin phase variation. To circumvent these drawbacks, in this study we instead

created phase-locked strains by mutating residues in the right inverted repeat predicted to be critical for flagellar switch inversion. We identified mutations that cause a partial or full attenuation of flagellar switch inversion, and *in vitro* characterization of these mutants showed a corresponding reduction or loss of flagellum and toxin phase variation. The locked ON and OFF mutants were assessed in hamster and mouse models of CDI for altered colonization, virulence properties, and toxin production. In a hamster model of acute CDI, the phase-locked mutants did not differ from wildtype in ability to cause disease and showed a modest defect in colonization, despite significant differences in toxin accumulation in the cecum between the locked-ON and -OFF mutants. In contrast, in a mouse model of CDI, the locked-ON mutant elicited significantly greater weight loss and maintained higher colonization levels compared to wildtype and the locked-OFF mutant. Differences were attributable at least in part to toxin levels achieved by these strains during infection. These results indicate that the capacity of *C. difficile* to phase vary flagellum and toxin biosynthesis during infection impacts its ability to colonize and cause disease *in vivo*.

Results

Identification of nucleotides in the right inverted repeat of the flagellar switch that are important for inversion

To determine the role of flagellum and toxin phase variation in *C. difficile* infection, we aimed to create mutants incapable of inverting the flagellar switch while avoiding the pleiotropic effects of inactivating *recV*. We focused on the flagellar switch inverted repeats (IRs), as these regions are typically directly recognized by the site-specific recombinase and important for switch inversion. To identify candidate nucleotides in the IRs required for inversion of the

flagellar switch by RecV, we performed an alignment of the IRs of the six RecV-invertible sequences in *C. difficile*. Although the invertible sequences differ in length and nucleotide sequence, the IRs share some sequence similarity suggesting that specific residues are important for interacting with RecV. Sequence conservation is strongest among the left inverted repeats (LIRs) of five invertible sequences and right inverted repeat (RIR) of the *cwpV* switch; lower identity is apparent among the respective RIRs (and LIR of *cwpV*) (Figure 1A).

We recently showed that the flagellar switch impacts gene expression in a mechanism acting after transcription initiation and occurring within the leader region of the *flgB* operon mRNA. While not fully elucidated, this regulation is dependent on Rho-mediated transcription termination that preferentially impacts *flg* OFF mRNA, a mechanism that requires Rho to interact with the mRNA either within or upstream of the flagellar switch.[41] To minimize the risk of interfering with Rho-mediated regulation, we chose to mutate the RIR downstream of the flagellar switch.

Because the starting orientation of an invertible element can impact the efficiency of inversion by a recombinase, both *flg* ON and *flg* OFF versions were created for each mutation. Three sites were selected for mutagenesis. First, we deleted 18 of the 21 bp of the *flg* RIR to create *flg*-ΔRIR ON and OFF mutant sequences, which we anticipated would prevent switch inversion;[43] however, the larger deletion presents greater risk of altering Rho-mediated regulation. Second, we chose three highly conserved CAA nucleotides in the *flg* RIR for substitution with GTT to create *flg*-3sub ON and OFF mutant sequences (Figure 1A). Third, we targeted the previously identified nucleotide where the DNA strand is cleaved by RecV to catalyze strand exchange (Figure 1A).[24] This residue and the two adjacent nucleotides were deleted to create *flg*-Δ3 ON and OFF mutant sequences.

Due to the challenges of creating unmarked chromosomal mutations in *C. difficile*, we first evaluated the effects of the RIR mutations on flagellar switch inversion using a previously described method employing *E. coli* as a heterologous host.[22, 23] In this assay, the *E. coli* strains bear two plasmids. One plasmid contains *recV* under the control of an anhydrotetracycline (ATc)-inducible promoter, and the other plasmid contains the target flagellar switch sequence.[23] Primers specific to each orientation of the switch are then used for detection by PCR. Each of these plasmid-borne target sequences was co-transformed into *E. coli* with pRecV, and the resulting strains were grown with or without ATc to induce *recV* expression then subjected to PCR with orientation-specific primers. As observed previously, only the starting orientation of the flagellar switch sequence was detected in the absence of *recV* induction with ATc for both *flg* ON and *flg* OFF constructs (Figure 1B, C, left). Upon induction with ATc, inversion of the wild-type flagellar switch sequence was detected, evident by the appearance of the *flg* OFF product from the *flg* ON target (Figure 1B, right) and the *flg* ON product from the *flg* OFF target (Figure 1C, right). The *flg*-3sub mutation appeared to reduce but not eliminate inversion by RecV, as the product for the inverted sequence remained detectable (Figure 1B, C, right). In contrast, no inversion was detected for the *flg*-ΔRIR and *flg*-Δ3 target sequences, regardless of the starting orientation of the flagellar switch (Figure 1B, C). The starting orientation of the flagellar switch did not affect invertibility of any of the target sequences by RecV in this assay. These data suggest that the *flg*-ΔRIR and *flg*-Δ3 mutations in the RIR render the flagellar switch into a "locked" state, while the *flg*-3sub mutation impairs flagellar switch inversion.

Loss of flagellar switch inversion in the RIR mutants leads to *C. difficile* phase-locked for motility and toxin production

We next sought to determine the effects of the RIR mutations on flagellar switch inversion and phase variation in *C. difficile*. We used allelic exchange to create six R20291 mutant strains: *flg*-3sub ON, *flg*-ΔRIR ON, *flg*-Δ3 ON, *flg*-3sub OFF, *flg*-ΔRIR OFF, and *flg*-Δ3 OFF. The process of generating strains with these precise mutations was facilitated by first deleting the 5'UTR region, then restoring that region with the desired nucleotide changes incorporated. These mutants were confirmed to have the expected flagellar switch orientation using quantitative PCR with orientation-specific primers (OS-qPCR) (Figure 1D). Each mutant contained the flagellar switch exclusively in the anticipated ON or OFF orientation (0 ± 0 % *flg* OFF for the *flg* ON mutants, 100 ± 0 % *flg* OFF for the *flg* OFF mutants) after growth in rich, liquid medium, in contrast to wildtype which exhibited heterogeneity (0.6 ± 0.3 % *flg* OFF).

To establish that these genetically locked mutants are also phenotypically locked, we first tested these strains in soft agar swimming motility assays. We found that, as expected, the wildtype and *flg* ON mutant strains (*flg*-ΔRIR, *flg*-Δ3, and *flg*-3sub) exhibited comparable motility (Figure 2A, B). In contrast, examination of the equivalent mutations in the *flg* OFF background revealed distinct effects of the mutations on flagellar phase variation. The *flg*-ΔRIR OFF and *flg*-Δ3 OFF mutants remained non-motile, equal to the nonmotile *sigD*-null control, indicating that these mutations prevent phase variation. However, the *flg*-3sub OFF mutant exhibited motility in this assay. These results are consistent with the data in Figure 1 indicating that the 3sub mutation reduces but does not eliminate flagellar switch inversion, and they suggest that the motility medium presented a selective pressure for the *flg* ON variants.

Because toxin gene expression is linked to transcription of the *flgB* operon via SigD,[38, 39] we evaluated toxin production in the *flg* RIR mutant strains. By immunoblot, the *flg*-ΔRIR, *flg*-Δ3, and *flg*-3sub ON strains produced TcdA at levels equivalent to the wildtype parent after

growth in TY broth (Figure 2C). TcdA was undetectable in the three *flg* OFF mutants, similar to the *sigD*-null control. Using a Vero cell rounding assay, which detects the activities of TcdA and TcdB, to quantify the toxin produced by these strains in broth culture, we found that the three *flg* OFF mutants and *sigD* control cultures contained significantly lower toxin titers than the *flg* ON mutants and wildtype (Figure 2C). Therefore, mutations in *flg* RIR that impede inversion of the flagellar switch concomitantly impact toxin production *in vitro*.

While a swimming motility assay can show the lack of flagellar switch inversion from OFF to ON in non-motile bacteria, it cannot detect inversion from ON to OFF in motile bacteria (including the *flg* ON RIR mutants) because the motile phenotype dominates in this assay. As an alternative way to determine whether the *flg*-3sub, *flg*-ΔRIR and *flg*-Δ3 ON mutants are capable of inversion, we assessed the effect of *recV* overexpression on flagellar switch inversion from ON to OFF using qPCR with orientation-specific primers (OS-qPCR). As seen previously, the wild-type R20291 populations were skewed toward the *flg* ON orientation, with less than 5% *flg* OFF cells, and expression of *recV* increased *flg* switch inversion resulting in a larger *flg* OFF population (Figure 2D).[23] The three *flg* ON RIR mutants bearing vector, with *recV* expressed at its natural levels, consisted of only *flg* ON bacteria (0% *flg* OFF, n=4). Despite *recV* overexpression, no *flg* OFF bacteria were detected in the *flg*-ΔRIR and *flg*-Δ3 ON mutants. However, overexpression of *recV* increased the subpopulation with the OFF orientation in the *flg*-3sub ON mutant, though potentially at a lower frequency than in the wildtype. Together with the *flg* OFF motility data and the *E. coli* inversion experiments, these results show that deletion of the RIR (ΔRIR) or three nucleotides at the site of recombination (Δ3) results in complete loss of flagellar switch inversion and phase variation, while a substitution of three conserved residues (3sub) reduces the frequency of inversion.

226

227 **Preventing flagellar switch inversion affects colonization and toxin accumulation in a**
228 **hamster model of infection**

229 *In vitro*, restricting inversion of the flagellar switch affects both motility and toxin
230 production. Because both characteristics are important during CDI, we analyzed the virulence of
231 *flg* RIR mutants in a hamster model of infection, which is particularly sensitive to TcdA and
232 TcdB and manifests acute CDI.[19, 20, 44] Prior work showed that inactivation of genes in the *flgB*
233 operon, which resulted in reduced toxin production, also attenuated virulence in this model,[32, 33]
234 so we anticipated that the hamster model would distinguish the virulence of phase-locked *flg* ON
235 and *flg* OFF mutants. To conserve animals, we narrowed this study to the *flg*-Δ3 mutants which
236 contain the smallest mutation that prevents flagellum and toxin phase variation. Antibiotic-
237 treated male and female Syrian golden hamsters were inoculated with 1000 spores of wild-type
238 R20291, *flg*-Δ3 ON, or *flg*-Δ3 OFF. These strains had no differences in growth (Figure S1),
239 germination (Figure S2), or sporulation (Figure S3) *in vitro*. The animals were monitored for
240 disease symptoms, including diarrhea and weight loss, and were euthanized if they exhibited
241 hallmarks of disease as detailed in Materials and Methods. Initially, hamsters infected with the
242 *flg*-Δ3 ON or *flg*-Δ3 OFF mutants appeared to become acutely symptomatic sooner than those
243 infected with wildtype, however, there were no significant differences in time to euthanasia for
244 animals infected with any of the strains (Figure 3A).

245 To determine bacterial burden, cecal contents collected immediately after euthanasia
246 were serially diluted and plated on taurocholate cycloserine cefoxitin fructose agar (TCCFA) to
247 enumerate *C. difficile* colony forming units (CFU). All animals that succumbed to disease had *C.*
248 *difficile* detectable in their cecal contents (10^4 CFU/g to 10^7 CFU/g). Wild-type R20291 was

present in 5.3-fold greater CFU compared to the *flg*-Δ3 ON mutant ($p < 0.01$); there were no significant differences among the other strains (Figure 3B). In the distal colons there was a similar trend, with 5-fold more CFU/g for the *flg*-Δ3 OFF mutant compared to the *flg*-Δ3 ON mutant ($p = 0.06$) (Figure 3C). These results suggest that flagellar phase-locked ON mutants are less fit than the phase-locked OFF mutants in the hamster intestinal tract, though the effect was modest.

Because of the link between production of flagella and toxins *in vitro*, we analyzed toxin titers in cecal contents of hamsters that succumbed to disease using the Vero cell rounding assay.[45] All samples from infected animals caused detectable cell rounding, while no cell rounding occurred when treated with diluted cecal contents from mock-inoculated animals. The toxin titers for the *flg*-Δ3 ON samples were 6.5-fold higher compared to the *flg*-Δ3 OFF ($p < 0.01$) (Figure 3D). These results indicate that, despite the lack of difference in ability to cause acute CDI, preventing phase variation led to significant differences in toxin accumulation during infection, and flagellum and toxin gene expression are linked during infection as observed *in vitro*.

Preventing flagellar switch inversion impacts colonization and disease dynamics of *C. difficile* in a mouse model

While the hamster models acute CDI, the mouse typically develops less severe disease and serves as a model of *C. difficile* colonization. Antibiotic-treated male and female C57BL/6 mice were inoculated with 10,000 spores of wild-type R20291, *flg*-Δ3 ON, or *flg*-Δ3 OFF.[46] Over the following 10 days, the mice were monitored for diarrhea and weight loss, and fecal samples were collected daily to assess bacterial burden and toxin levels. Bacterial burden in

feces achieved the highest levels between days 1 and 4 post-inoculation (p.i.) (Figures 4A, S4). Although all three strains were present in equivalent numbers during this time frame, the *flg*-Δ3 ON elicited significantly greater weight loss than *flg*-Δ3 OFF on days 1 through 3 (Figures 4C, S5). Wildtype resulted in intermediate weight loss, with significant differences from *flg*-Δ3 ON and *flg*-Δ3 OFF on days 2 and 3 p.i. (Figure 4D). The WT- and *flg*-Δ3 ON-infected mice began recovering weight on day 3 p.i., with no significant differences in weight loss among the groups on day 4 and later. On day 4 p.i., the CFU/g feces from wildtype and *flg*-Δ3 OFF infected mice began to decline, often to below the limit of detection, while *flg*-Δ3 ON showed a comparatively modest decline between days 3 and 4 and then was maintained at ~10^5 CFU/g feces in all mice through the duration of the experiment (Figures 4A, 4B, S4).[41] The *flg*-Δ3 ON mutant was present in significantly higher numbers than wildtype on days 6 through 10 p.i. (Figures 4A, S4). The *flg*-Δ3 OFF mutant colonized to levels similar to wildtype or intermediate between wildtype and *flg*-Δ3 ON.

We additionally ensured that *flg*-Δ3 ON and *flg*-Δ3 OFF remained phase-locked by evaluating them at the infection endpoint. OS-qPCR analysis of genomic DNA purified from fecal samples indicated that the flagellar switch remained locked in *flg*-Δ3 ON (collected on day 9 p.i.; data not shown). The lower colonization levels by *flg*-Δ3 OFF after day 5 precluded OS-qPCR analysis. As an alternative approach, *flg*-Δ3 OFF bacteria from day 9 fecal samples were cultured on TCCFA, then *C. difficile* growth was pooled and tested for swimming motility. No motility was observed, suggesting that the flagellar switch remained in the OFF orientation and that no motile suppressor mutants arose during infection (data not shown). Together these results indicate that preventing flagellar switch inversion impacts *C. difficile* colonization and disease

294 symptom development, with the locked-ON state resulting in greater disease (weight loss) and
295 maintenance of colonization.
296
297 **Differences in weight loss is attributable to a higher accumulation of toxins in *flg*-Δ3 ON**
298 **infected mice**
299 Differences in weight loss between mice infected with the *flg*-Δ3 ON compared to
300 wildtype and *flg*-Δ3 OFF are consistent with the differences in toxin production by these strains.
301 However, the weight recovery observed in mice infected with *flg*-Δ3 ON indicated that this strain
302 may have decreased toxin production through a SigD-independent mechanism. To evaluate this
303 possibility, we determined the toxin titers in fecal samples collected over the 10-day experiments
304 using a Vero cell rounding assay (44). All samples from infected animals caused detectable cell
305 rounding, while no cell rounding occurred when treated with samples from mock-inoculated
306 animals. On day 2, when the differences in weight loss between groups are greatest, the toxin
307 titers in feces collected from *flg*-Δ3 ON-infected mice were significantly higher than from mice
308 infected with wildtype ($p = 0.0041$); toxin titers were also higher than in feces from *flg*-Δ3 OFF-
309 infected mice, though the differences did not reach statistical significance (Figure 4E). No
310 significant differences in toxin titers between groups of animals were observed for days 4 and 6.
311 On day 8, the *flg*-Δ3 ON samples again had toxin titers higher compared to the wildtype samples
312 ($p < 0.05$) (Figure 4E). These results suggest that the differences in weight loss observed on day
313 2 p.i., when bacterial burden was equivalent across groups of infected animals (Figure 4C), is
314 attributable at least in part to a higher accumulation of toxins in mice infected with *flg*-Δ3 ON.
315 However, the higher toxin levels in *flg*-Δ3 ON-infected mice at later stages are likely due to the
316 higher bacterial burden for this strain.

Discussion

In this study, we used precisely engineered mutations to the right inverted repeat to restrict flagellar switch inversion in *C. difficile* R20291, which allowed us to determine the role of flagellum and toxin phase variation in *C. difficile* physiology *in vitro* and during infection in two rodent models. We characterized mutants with varying abilities to undergo flagellar switch inversion and therefore flagellum and toxin phase variation. *In vitro*, these mutants were either attenuated or fully genotypically and phenotypically locked for swimming motility and toxin biosynthesis but were indistinguishable from wild-type bacteria in growth, sporulation, and germination rates. We analyzed phase-locked mutants in hamster and mouse models of *C. difficile* infection, with distinct outcomes. In hamsters, while the phase-locked mutants led to accumulation of significantly different levels of toxins in the cecum, these differences did not impact acute disease development. In contrast, in the mouse model the mutant with the flagellar switch locked in the ON state caused greater weight loss and persisted longer than wildtype and the locked OFF mutant, which is attributable to higher toxin levels produced by the locked-ON strain in vivo. These findings indicate that the ability to undergo flagellar switch inversion impacts *C. difficile* colonization and disease development.

Previous studies showed that the site specific recombinase RecV is required for inversion of the *flg*, *cwpV*, *cmrRST*, and CDR20291_0963 switches, and over-expression of *recV* influences the inversion of the CDR20291_0685 and CDR20291_1514 switches.[24, 42] Interestingly, the inverted repeats for a given invertible sequence vary in length and in position relative to the determined site of DNA recombination.[24] Further, sequence conservation among the inverted repeats of RecV-invertible sequences is modest, making the identification of a core

RecV-binding sequence difficult. We found that substitution of three residues that are conserved among most of the RIRs (*flg*-3sub) reduced flagellar switch inversion from ON to OFF and OFF to ON but did not eliminate inversion. However, deleting the residue previously determined to be the site of flagellar switch inversion in the RIR and the two flanking residues (*flg*-Δ3), prevented inversion as effectively as deleting the RIR. These results validate the approach of identifying the recombination site by evaluating enrichment of 5' end clipped reads generated by whole genome sequencing.[24] Future work will determine whether changes to the site of recombination impair RecV binding and/or the ability to catalyze DNA inversion.

The *C. difficile flg* RIR mutants served to assess the role of flagellar switch inversion on phase variation *in vitro* and *in vivo*. The *flg*-Δ3 and *flg*-ΔRIR mutations resulted in genetically and phenotypically locked strains. The respective ON mutants were motile while the OFF mutants remained non-motile. Consistent with the previously characterized link between flagellum and toxin gene expression via SigD, the ON mutants produced significantly more toxins *in vitro* than the OFF mutants, which produced toxins at a level comparable to the *sigD* control. In contrast to these RIR mutations, the *flg*-3sub mutation appeared to reduce but not eliminate flagellar switch inversion – the inversion assay using *E. coli* showed inversion levels intermediate between the WT and the *flg*-Δ3/*flg*-ΔRIR sequences. In a soft agar swimming motility assay, the *flg*-3sub OFF mutant exhibited motility, possibly because this assay imposes a strong selective pressure for bacteria that can swim to access nutrients;[41] the *flg*-3sub OFF bacteria that phase varied to *flg* ON would possess an advantage and lead to the observed motile phenotype. Consistent with the swimming motility medium imposing a selective pressure, motile suppressor mutants appeared in some experiments testing the swimming motility of the *flg*-ΔRIR and *flg*-Δ3 OFF mutants, as we observed previously for the *recV flg* OFF mutant.[41] Unlike in the

363 motility assays, no difference in toxin level was apparent between the *flg*-3sub OFF and the *flg*-
364 ΔRIR and *flg*-Δ3 OFF mutants, likely because the growth conditions for the toxin experiments
365 did not present a selective pressure for the *flg* ON variants.

366 Prior work by Aubry et al. using the hamster model of acute CDI showed that mutation of
367 genes in the *flgB* operon in *C. difficile* 630Δ*erm* resulted in reduced toxin gene expression,
368 reduced toxin production, and attenuated virulence in hamsters.[32] Our results showing no
369 discernable difference in CDI development in hamsters between R20291 phase-locked ON and
370 OFF mutants were therefore unexpected. The discrepancy in results may be attributable to strain
371 background. We used 027 ribotype *C. difficile* R20291, which expresses toxin genes and
372 produces toxins at higher levels than the 630 lineage.[36, 47] There are known differences in the
373 flagellar loci in 630 and R20291 strains,[36] and we previously showed that *C. difficile* 630 is not
374 capable of flagellum and toxin phase variation.[25] In addition, mutation of flagellar genes had
375 different effects in R20291 and 630Δ*erm*, a derivative of 630.[32, 33, 48] We suspect that, despite
376 exhibiting ~6-fold reduced toxin accumulation compared to the other strains, *flg*-Δ3 OFF
377 nonetheless secreted sufficient toxin to cause acute disease in hamsters given their high
378 sensitivity to *C. difficile* toxins.

379 Flagella have been shown to play a contributing role in R20291 colonization of the
380 mouse intestinal tract. Non-motile R20291 *fliC* (flagellin), *fliD* (flagellar cap), or *flgE* (hook
381 protein) mutants showed reduced adherence to Caco-2 intestinal epithelial cells *in vitro*, and in a
382 co-infection with wild-type R20291, the *fliC* mutant colonized mice in fewer numbers.[33] In the
383 current study, the mouse model was more effective at revealing differences between *flg*-Δ3 ON
384 and *flg*-Δ3 OFF. During peak colonization on days 1-3 p.i., *flg*-Δ3 ON resulted in the greatest
385 weight loss, consistent with higher toxin production by this mutant *in vitro*; *flg*-Δ3 OFF did not

386 elicit weight loss in mice, despite being present in equivalent numbers at these time points and
387 producing toxin levels similar to wildtype. During later stages of infection, most mice began
388 recovering weight between days 3 and 4 p.i., when bacterial loads begin to decline, and weights
389 were indiscernible from mock-inoculated animals by day 6. Interestingly, mice infected with *flg*-
390 Δ3 ON recovered their starting weight, even though their numbers were 2-logs higher than
391 wildtype and *flg*-Δ3 OFF. One possible explanation for weight recovery in *flg*-Δ3 ON-infected
392 mice is a SigD-independent (and therefore phase variation independent) down-regulation of
393 toxin production. For example, another toxin gene regulator such as CcpA or CodY could limit
394 toxin synthesis, and SigH, Spo0A, RstA, and SinR could also unlink flagellar and toxin gene
395 expression.[49-53]. However, mean toxin titers remained consistent in feces from *flg*-Δ3 ON-
396 infected mice (compared to decreasing titers from wildtype and *flg*-Δ3 OFF-infected mice). The
397 lack of weight loss in *flg*-Δ3 OFF-infected mice at early time points and in *flg*-Δ3 ON-infected
398 mice at later stages could be due to altered localization of these phase-locked mutants in the
399 intestinal tract, which we speculate results in inefficient delivery of toxins to the epithelium.
400 Both flagellin and the toxins of *C. difficile* have marked immunostimulatory properties and
401 exhibit cooperativity in eliciting an inflammatory response,[18, 54-56] which may alter the spatial
402 and temporal dynamics of colonization for a strain with constitutively elevated (*flg*-Δ3 ON) or
403 reduced (*flg*-Δ3 OFF) levels of these factors. It is also possible that the observed phenotypes are
404 driven by other mechanisms. SigD, encoded in the *flgB* operon and regulated by the flagellar
405 switch, also regulates genes involved in membrane transport, metabolism, regulation, and cell
406 wall protein synthesis.[39] These factors may therefore be subject to phase variation and influence
407 *C. difficile* colonization and pathogenesis.

Beyond the population-level analyses of the current study, future work investigating the spatial and temporal dynamics of colonization by individual *flg* ON and *flg* OFF cells, both phase-locked and those arising in a wild-type background, may help clarify the effects of flagellum and toxin phase variation on *C. difficile* colonization and disease development. Does one variant population appear in a particular region of the intestine, either longitudinally or with respect to the epithelium? Does one variant associate with sites of inflammation? Such studies may reveal host and microbiota-derived factors that influence the fitness and virulence of *C. difficile*. Further, because these variants exhibiting different disease potential arise naturally and switch stochastically, flagellum and toxin phase variation may influence not only disease severity but also recurrence. This work may therefore help to identify the *C. difficile* determinants of infection versus asymptomatic carriage which may in turn lead to strategies to distinguish between these potential outcomes, better predict disease severity and recurrence, and mitigate transmission.[57]

Materials and Methods

Growth and maintenance of bacterial strains

Strains and plasmids used in this study are listed in Table S1. *C. difficile* strains were grown in an anaerobic chamber (Coy Laboratories) using a gas mix consisting of 85% N_2, 5% CO_2, and 10% H_2. *C. difficile* was routinely cultured in Brain Heart Infusion medium (Becton Dickinson) supplemented with 5% yeast extract (Becton Dickinson) (BHIS) or in Tryptone Yeast (TY) broth as indicated. All *C. difficile* broth cultures were grown at 37°C statically, with 10 µg/mL thiamphenicol (Tm_{10}) for plasmid maintenance as needed. *E. coli* DH5α and HB101(pRK24) were cultured under aerobic conditions in LB broth, Miller (Fisher) at 37°C. In

E. coli, plasmids were maintained with 100 µg/mL ampicillin (Amp_{100}), 10 µg/mL chloramphenicol (Cm_{10}), and/or 100 µg/mL kanamycin (Kan_{100}), as indicated.

Orientation-specific PCR

E. coli strains used in this study are listed in Table S1. Strains used for orientation-specific PCR contain two plasmids: one for expression of *recV* and the other containing the target flagellar switch sequence.[22, 23] Bacteria were subcultured in BHIS-Cm_{10}-Kan_{100} overnight at 37°C and diluted 1:50 into fresh medium. When cultures reached an OD_{600} 0.3-0.4 (early exponential phase), 200 ng/ml anhydrotetracycline (ATc) was added to induce *recV* expression. Cultures were grown until OD_{600} 1.0, and plasmids were purified using the GeneJET Plasmid Miniprep Kit (Thermo Fisher). Purified plasmids were used as template for PCR using primers that discriminate between each flagellar switch sequence orientation. Primers R1614 and R857 were used to amplify the ON orientation of the flagellar switch, which corresponds to the published sequence of R20291 (FN545816.1). Primers R1615 and R857 were used to amplify the OFF orientation of the flagellar switch. All primer sequences are listed in Table S2.

Generation of mutant strains

To facilitate the generation of mutations in the *flgB* UTR in *C. difficile* R20291, we first deleted the UTR then restored the region with mutant versions of the sequence by allelic exchange with pMSR0, an *E. coli-C. difficile* shuttle vector for toxin-mediated allele exchange mutagenesis.[58] To delete the *flgB* UTR (*flgB*ΔUTR), upstream and downstream homology regions were amplified from R20291 genomic DNA with R2459 and R2448 or R2449 and R2450, respectively. Gibson assembly was used to introduce these fragments into BamHI-

454 digested pMSR0. Clones were confirmed by PCR and sequencing with plasmid-specific primers
455 R2743 and R2744, which flank the cloning site. The resulting plasmid pRT2546 was introduced
456 into heat-shocked *C. difficile* R20291 via conjugation with *E. coli* HB101(pRK24).[59] The
457 procedure for allelic exchange was performed as described previously,[58] except transconjugants
458 were selected and passaged on BHIS-Tm_{10}-Kan_{100} agar. Individual colonies were streaked on
459 BHIS-Tm_{10}-Kan_{100} agar to ensure purity, then streaked on BHIS-agar with 100 ng/ml ATc
460 (ATc_{100}) to induce expression of the toxin-antitoxin genes and eliminate bacteria that still contain
461 pMSR0. Colonies were screened for the desired deletion by PCR with R2451 and R2452.
462 Genomic DNA was isolated from presumptive mutants, amplified with R2451 and R2452, and
463 the resulting PCR product was sequenced with R1512 and R2672 to confirm integrity of the
464 sequence.

465 Six different inverted repeat mutant constructs were created in *C. difficile flgB*ΔUTR. For
466 all three *flg* ON constructs, RT1702 (*recV flg* ON) genomic DNA was used as the template, and
467 RT1693 (*recV flg* OFF) was used as the template for all three *flg* OFF constructs. Mutants with 3
468 nucleotide substitutions (*flg*-3sub) were created by changing nucleotides 440-442 of the 498 nt
469 *flgB* UTR from CAA to GTT (Figure 3.2). Mutants with deletions of the right inverted repeat
470 (*flg*-ΔRIR) had nucleotides 424-442 of the *flgB* UTR deleted. A 3 bp deletion (*flg*-Δ3) was made
471 by deleting nucleotides 424-426 of the *flgB* UTR. Overlapping PCR fragments with the desired
472 mutation were amplified and introduced into BamHI/XhoI-digested pMSR0 by Gibson
473 assembly. The following primer pairs were used to amplify the respective fragments (designated
474 as upstream, downstream): *flg*-3sub OFF – R2896 and R2883, R2882 and R2843; *flg*-ΔRIR OFF
475 – R2896 and R2870, R2869 and R2843; *flg*-Δ3 OFF – R2896 and R2885, R2884 and R2843; *flg*-
476 3sub ON – R2896 and R2889, R2888 and R2843; *flg*-ΔRIR ON – R2896 and R2887, R2886 and

R2843; *flg*-Δ3 ON – R2896 and R2891, R2890 and R2843. The presence of inserts in pMSR0 was confirmed by PCR with R2743 and R2744, and desired mutations were confirmed by sequencing with R1611, R2313 and R2314. The resulting pMSR0 derivatives were introduced into the *flgB*ΔUTR mutant by conjugation with *E. coli* HB101(pRK24). After selection on BHIS-ATc$_{100}$ plates, colonies were screened with R1512 and R1611 for integration of *flg* constructs. Genomic DNA was isolated from presumptive mutants, amplified with R2451 and R2452, and the resulting PCR product was sequenced with R1512 to confirm integrity of the sequence. The *flg*-Δ3 mutants used in the infection studies and parental R20291 strain were subjected to whole genome sequencing (Microbial Genome Sequencing Center, Pittsburg, PA) to confirm that no unintended sequence polymorphisms arose.

To generate inverted repeat mutants in *E. coli*, the mutant constructs were amplified from the respective pMSR0 plasmids (OFF – *flg*-3sub, *flg*-ΔRIR, *flg*-Δ3; ON – *flg*-3sub, *flg*-ΔRIR, *flg*-Δ3) using R1512 and R1611. These constructs were digested with SphI/EcoRI and ligated into similarly digested pMC123. The presence and integrity of insert was confirmed by PCR with R2313 and R2314 and by sequencing with R2313 and R2462 for *flg* ON and R313 and R2463 for *flg* OFF versions. For inversion assays in *E. coli*, these constructs were co-transformed with pMWO-074::*recV* (ATc-inducible P_{tet} promoter) into DH5α.

For overexpression of *recV* in *flg* ON inverted mutant strains, pRT1611 (vector control) or pRT1611::*recV* were introduced by conjugation with *E. coli* HB101(pRK24) and confirmed by PCR.

Quantitative PCR analysis of the flagellar switch orientation in C. difficile

C. difficile strains were grown in BHIS medium to an OD_{600} ~1.0, and genomic DNA was extracted as previously described.[60] To analyze flagellar switch orientation from *C. difficile* in mouse feces, fecal samples were suspended in DPBS, treated with lysozyme, and subjected to bead beating to lyse cells including spores. Genomic DNA was purified by phenol/chloroform extraction and washed with ethanol. Quantitative PCR was done using 10 ng (broth culture) or 100 ng (fecal samples) of genomic DNA as template with SYBR Green Real-Time qPCR reagents (Bioline), primers at a final concentration of 1 µM, and an annealing temperature of 55°C. Primers R2175 and R2177 were used to detect the ON orientation and primers R2176 and R2177 were used to detect the OFF orientation. Quantification was done as described previously using the *rpoC* as the control gene.[24]

Swimming motility assay

For assays using *in vitro* cultures, a single colony from a freshly streaked BHIS plate was inoculated into 0.5X BHIS-0.3% agar to assay flagellum-dependent swimming motility as previously described.[37] The diameter of motile growth was measured after 48 hours incubation at 37°C. Plates were imaged using the G:BOX Chemi imaging system with the Upper White Light illuminator. To assess swimming motility of *C. difficile* present in mouse feces, diluted fecal samples from each were plated on TCCFA to enrich for *C. difficile*, and growth was pooled and tested for swimming motility in 0.5X BHIS-0.3% agar.

Detection of TcdA by immunoblot

Immunoblot for TcdA production was performed as previously described.[23, 41, 61] Cultures were grown overnight (~16 hours) in TY broth, normalized to an OD_{600} 1.0, and collected by

centrifugation at 16,000 x g for 5 minutes. Pellets were suspended in 2x SDS-PAGE sample buffer and boiled for 10 minutes. Samples were electrophoresed on 4%–15% Mini-PROTEAN TGX Precast Protein Gels (Bio-Rad) and transferred to a nitrocellulose membrane (Bio-Rad). Membranes were stained with Ponceau S (Sigma) to assess sample loading and imaged using the G:Box Chemi imaging system. TcdA was detected using mouse α-TcdA antibody (Novus Biologicals) followed by goat anti-mouse IgG secondary antibody conjugated to DyLight 800 4x PEG (Invitrogen). Blots were imaged using the Odyssey imaging system (LI-COR).

Vero cell rounding assay

We used a previously described protocol to quantify *C. difficile* toxin activity in hamster cecal contents, mouse feces, and bacteria grown overnight in TY broth.[45] For the assay, $5x10^4$ Vero cells in 90 µl were seeded in each well of a tissue-culture treated, flat bottom 96-well plate (Corning) and allowed to incubate overnight (~24 hours). The following day, cecal contents collected during necropsy (hamsters) or fecal samples (mice) were thawed at room temperature, weighed, and suspended in 1x DPBS to make an initial 1:10 dilution stock. *In vitro* cultures were grown overnight (~16 hours) in TY broth, OD_{600} was measured, and cells were pelleted by centrifugation at 16,000 x g for 5 minutes. Supernatants of cecal contents, fecal samples, and broth cultures were sterilized by passing through a 0.45 µm filter. Serial dilutions in 1x DPBS were performed on ice, and 10 µl were applied to each well with Vero cells. DPBS was used as a control. The cells were incubated overnight (~18 hours) in a tissue culture incubator at 37ºC and an atmosphere with 5% CO_2, and cell rounding was assessed using a 10x objective on a light microscope. Toxin titer was calculated as the reciprocal of the highest dilution causing ≥80% cell rounding, normalized to OD_{600} of the starting culture (*in vitro*), the amount of cecal contents, or

545 the amount of fecal material (*in vivo*). Samples collected from mock-infected animals were also
546 assayed to show that rounding was specific to *C. difficile*-infected animals.
547
548 ***Spore purification***
549 Overnight cultures (100 µL) were spread on three to five 70:30 agar plates.[62] After 72
550 hours of growth at 37°C, bacterial growth was collected, suspended in 10 mL DPBS and stored
551 aerobically at room temperature overnight. Spores were purified by washing the suspension four
552 times with DPBS before purification using a sucrose gradient as described.[63] After discarding
553 supernatant that contains cell debris, the spore pellet was washed five more times with DPBS +
554 1% BSA. Spores were stored in DPBS + 1% BSA at room temperature until use.
555
556 ***Sporulation assay***
557 Sporulation was assayed as described previously.[64] Briefly, *C. difficile* strains were
558 grown overnight in BHIS medium supplemented with 0.1% TA and 0.2% fructose to prevent
559 spore accumulation. Cultures were diluted 1:30 in BHIS-0.1% TA-0.2% fructose and upon
560 reaching OD_{600} 0.5, 250 µl of culture was applied to 70:30 agar [62]. An ethanol resistance
561 sporulation assay was performed at this point to confirm the absence of spores at the initiation of
562 the assay. After 24 hours of growth at 37°C, cells were suspended in BHIS to an OD_{600} 1.0, and
563 an ethanol resistance assay was performed. To eliminate all vegetative cells, 0.5 mL of culture
564 was mixed with 0.5 mL of 57% ethanol to achieve a final concentration of 28.5% ethanol,
565 vortexed and incubated for 15 minutes. To enumerate spores, serial dilutions were made in PBS-
566 0.1% TA and plated on BHIS-0.1% TA agar. To enumerate vegetative cells, serial dilutions of

the BHIS cell suspension were plated on BHIS agar. Sporulation efficiency was calculated as the total number of spores divided by the total number of viable cells (spores plus vegetative).

Germination assay

Spore germination was analyzed at room temperature (27°C) by measuring the change in OD_{600} as previously described.[65] The germination assay was performed in clear 96-well flat bottom plates (Corning) in a final reaction volume of 100 µl in buffer with 30 mM glycine, 50 mM Tris, 100 mM NaCl, pH 7.5. Spores were suspended in assay buffer, heated at 65°C for 30 minutes, placed on ice for 1 minute and added to wells to a final OD_{600} 0.7. At the start of the assay, 10 mM sodium taurocholate (Sigma Aldrich) (TA) was added to induce germination; no-taurocholate controls were done in parallel. Optical density was measured every 2 minutes for 1 hour using a BioTek Synergy plate reader.

Ethics statement

Mouse and hamster experiments were performed under the guidance of veterinary staff within the University of North Carolina Chapel Hill Division of Comparative Medicine (DCM). All animal studies were done with prior approval from UNC-CH Institutional Animal Care and Use Committee. Animals that were considered moribund were euthanized by CO_2 asphyxiation and thoracotomy in accordance with the Panel on Euthanasia of the American Veterinary Medical Association.

Animal Experiments

589 Hamster Experiments: Male and female six- to ten-week-old Syrian golden hamsters
590 (Charles River Laboratories) were housed individually and given a standard rodent diet and
591 water *ab libitum*. To induce susceptibility to *C. difficile* infection, one dose of clindamycin (30
592 mg/kg of body weight) was administered by oral gavage 5 days prior to inoculation. Hamsters
593 were inoculated by oral gavage with approximately 1,000 spores of a single strain of *C. difficile.*
594 Mock inoculated animals were included in each experiment. Fecal samples were collected daily
595 to examine bacterial burden. The animals were monitored at least daily for disease symptoms
596 including weight loss, diarrhea, wet tail, and lethargy. Hamsters that lost 15% or more of their
597 weight or showed severe signs of disease were euthanized by CO_2 asphyxiation and
598 thoracotomy. Immediately following euthanasia, a necropsy was performed, and cecal contents
599 (not cecal tissue) were collected for enumeration of bacterial CFU, genomic DNA isolation for
600 PCR, and toxin quantification. To enumerate CFU from fecal and cecal contents, samples were
601 weighed, suspended in 1 mL DPBS, heated at 55˚C for 20 minutes, and dilutions plated on
602 TCCFA.[66, 67] To enumerate CFU from the distal colon, the last 3 cm of the colon were excised
603 during necropsy. The samples were weighed, suspended in DPBS, processed with a tissue
604 homogenizer, heated, and plated similarly to cecal and fecal samples. *C. difficile* CFU were
605 enumerated after 48 hours of incubation. Twelve animals (6 male, 6 female) per *C. difficile* strain
606 were tested in two independent experiments. Log rank test for trend was used for statistical
607 analysis of survival data.
608 Mouse experiments: Groups of male and female C57BL/6 mice (Charles River
609 Laboratories) aged 8- to 10-weeks were subjected to a previously described antibiotic regimen to
610 render them susceptible to *C. difficile* infection.[46, 68] Mice were given a cocktail of kanamycin
611 (400 μg/ml), gentamicin (35 μg/ml), colistin (850 units/ml), vancomycin (45 μg/ml), and

metronidazole (215 μg/ml) in their water *ad libitum* seven days prior to inoculation for three days, then returned to regular water for the duration of the experiments. A single intra-peritoneal dose of clindamycin (10 mg/kg body weight) was administered 2 days prior to inoculation. Mice were randomly assigned into groups, with two mice assigned to the mock condition and six mice (3 male, 3 female) to each infection condition. The experiment was independently repeated, and the data were combined for a total of 12 mice (6 male, 6 female) in each infection condition. Mice were inoculated with 10^5 spores by oral gavage. Mock-inoculated animals were included as controls. Cage changes were performed every 48 h post-inoculation.[68, 69] Animal weights were recorded, and fecal samples were collected every 24 h for seven days post-inoculation. Fecal samples were homogenized, and dilutions were plated on TCCFA plates, which contain 0.1% of the germinant taurocholate to enumerate spores as colony forming units (CFU) per gram of feces. Additional fecal samples were collected for OS-qPCR analysis to determine flagellar switch orientation and for Vero cell rounding assays to quantify toxins.

Statistical Analysis and Data Availability

All experiments reflect at least three independent biological replicates, except for animal experiment, which were done twice. Statistical analysis was done using GraphPad Prism 9.1.0. Upon publication, the data that support the findings of this study are available from the corresponding author, R.T., upon reasonable request.

Acknowledgements

The authors declare no competing interests for this study. This work was supported by NIH award R01-AI107029 and R01-AI143638 to R.T. CLW is supported by an Institutional Research

635 and Academic Career Development Awards (IRACDA) fellowship under K12-GM000678. The
636 funding agency had no role in the design or execution of this study, the analysis of the data, or
637 the decision to publish the results.

Figure Captions

Figure 1. Mutations in *flg* RIR affect inversion in *E. coli* and *C. difficile*. A. Alignment of inverted repeats flanking the invertible DNA sequences affected by RecV. Shading denotes residues conserved in at least 4 of the 6 repeats. Putative inverted repeats are underlined. Hyphens between LIRs and RIRs represent the intervening sequences, which vary in length and nucleotide sequence. For the *flgB*-RIR, the site of cleavage by RecV is indicated with an asterisk. This nucleotide and the two adjacent residues, indicated in red, were deleted in *flg*-Δ3 constructs/strains. Note that the adenine 5' of the cleavage site is present in the *flg* ON sequence, whereas a thymine is present in *flg* OFF; constructs for mutagenesis were created in both *flg* orientations. The conserved CAA nucleotides mutated in *flg*-3sub constructs/strains are boxed in black. Nucleotides deleted in *flg*-ΔRIR bacteria/constructs are indicated. LIR, RIR = left, right inverted repeats. Numbers indicate locus tags in *C. difficile* R20291. B, C. Orientation-specific PCR to examine flagellar switch inversion in *E. coli* bearing wild-type or mutated inverted repeat target sequences. The starting orientation of the flagellar switch is indicated: *flg* ON (B) or *flg* OFF (C). Absence or presence of ATc for induction of *recV* expression is shown (-ATc/+ATc). The *flg* ON and *flg* OFF products are indicated with white and black arrows, respectively. Shown are representative images of three independent experiments. (D) Analysis of flagellar switch orientation in *C. difficile* RIR mutants by quantitative orientation-specific PCR. Means and standard deviations for three biological replicates are shown.

Figure 2. Mutations in *flg* RIR affect *C. difficile* motility and toxin production. (A) Representative image of swimming motility in soft agar medium of *C. difficile* R20291 (WT), *flg*-3sub ON and OFF, *flg*-ΔRIR ON and OFF, and *flg*-Δ3 ON and OFF, and *sigD*-null non-motile control, incubated for 48 hours. (B) Quantification of swimming motility after 48 h of

strains in (A). (C) Immunoblot detection of TcdA and toxin titers after growth in TY broth. For immunoblot, a representative image of three independent experiments is shown. Toxin titers of supernatants from overnight bacterial cultures were calculated as the reciprocal of the highest dilution that causes ≥80% rounding of Vero cells, expressed after log-transformation and normalization to OD_{600} of the cultures. (B, C) Each symbol represents one biological replicate, and dotted line represents the limit of detection. *p<0.05 by one-way ANOVA with Dunnett's post-test comparing values to *flg*-Δ3 ON. (D) Quantitative orientation-specific PCR of the flagellar switch in WT, *flg*-3sub ON, *flg*-ΔRIR ON, and *flg*-Δ3 ON mutants expressing *recV* (pRecV) or bearing vector. Means and standard deviations are shown. ****p<0.0001, ***p<0.001, **p<0.01 by one-way ANOVA and Dunnett's post-test comparing values to WT pRecV. P value for comparison of WT pRecV and *flg*-3sub ON pRecV was determined by unpaired two-tailed t-test. (B-D) Means and standard deviations are shown.

Figure 3. Interfering with flagellar switch inversion affects toxin accumulation and bacterial burden in a hamster model of CDI. Antibiotic-treated male and female Syrian Golden hamsters were inoculated with 1000 spores of wild-type R20291 (WT), *flg*-Δ3 ON, and *flg*-Δ3 OFF. Mock-inoculated animals were included in each experiment. Data are combined from two independent experiments testing strains in 3 male and 3 female hamsters, for 12 total hamsters per strain. (A) Kaplan-Meier analysis of survival. (B) CFU in cecal contents. **p<0.01 by Kruskal-Wallis test with Dunn's post-test. (C) CFU from homogenized distal colon from six animals of one experiment. P value was determined by Mann-Whitney test. (D) Toxin titers in cecal contents calculated as the reciprocal of the highest dilution to cause ≥80% rounding of Vero cells. No cell rounding occurred when treated with diluted cecal contents from mock-inoculated animals. Bars indicate the means; dotted line represents the limit of detection.

684 $^{**}p<0.01$ with Kruskal-Wallis test with Dunn's post-test. (B, C, D) Symbols indicate CFU from
685 individual animals and bars indicate medians.

686 **Figure 4. Locking the flagellar switch in the ON orientation exacerbates disease and**
687 **increases persistence of *C. difficile* in a mouse model of CDI.** Antibiotic-treated male and
688 female C57BL/6 mice were inoculated with 100,000 spores of wild-type R20291 (WT), *flg*-Δ3
689 ON, and *flg*-Δ3 OFF. Mock-inoculated animals were included in each experiment. Data are
690 combined from two independent experiments testing strains in 3 male and 3 female mice, for 12
691 total mice per strain. (A) CFU enumerated in fecal samples collected every 24 hours post-
692 inoculation (p.i.). Asterisks indicate statistical comparison to WT data at that time point. (B)
693 CFU per gram feces collected on day 6 p.i.; data for days 5 - 10 shown in Figure S4. Symbols in
694 each group distinguish results from two independent experiments. (C) Animal weights
695 determined every 24 hours post-inoculation, expressed as a percentage of the mouse's weight at
696 day 0. Asterisks indicate statistical comparison to mock data at that time point. (D) Animal
697 weights at Day 2 p.i.; data for days 1 - 6 shown in Figure S5. (E) Toxin titers in fecal samples
698 calculated as the reciprocal of the highest dilution to cause ≥80% rounding of Vero cells. No cell
699 rounding occurred when treated with diluted fecal contents from mock-inoculated animals. (A-E)
700 Symbols indicate values from individual animals; dotted lines represent limit of detection. (A, B,
701 E) Bars indicate the medians. Statistical significance was determined using the Kruskal-Wallis
702 test and Dunn's post-test. (C, D) Bars indicate means and standard error. Statistical significance
703 was determined by one-way ANOVA with Tukey's post-test. $^{*}p<0.05$, $^{**}p<0.01$, $^{***}p<0.001$,
704 $^{****}p<0.0001$.

705

706

Supporting information

Table S1. Strains and plasmids used in this study.

Table S2. Oligonucleotides used in this study.

Figure S1. Mutations in *flg* RIR do not affect growth. Growth curves of WT, *flg* ON and OFF RIR (3sub, ΔRIR, Δ3) mutants. Overnight cultures grown in TY medium were diluted 1:50 into BHIS broth. Optical density (OD_{600}) was measured every 30 minutes for 8 hours. Shown are the means and standard deviation for 6 biological replicates.

Figure S2. Mutations in *flg* RIR do not affect germination. Purified spores of indicated strains were germinated in the presence of taurocholate (+) or in buffer without germinant as a control (-), and optical density (OD_{600}) was measured. Germination was plotted as the ratio of optical density (OD_{600}) at a given time point (t_x) versus initial OD_{600} (t_0). A representative germination plot of six independent experiments each consisting of 2 technical replicates is shown.

Figure S3. Mutations in *flg* RIR do not affect sporulation. Sporulation efficiency was evaluated by ethanol resistance and calculated as the total number of spores divided by the total number of viable cells (spores plus vegetative). A sporulation-deficient *spo0A* mutant was included as a control. The means and standard deviation of three independent experiments are shown. n.d. – not detectable.

Figure S4. Bacterial load in feces collected from mice inoculated with WT, *flg*-Δ3 ON, and *flg*-Δ3 OFF. CFU enumerated in fecal samples collected every 24 hours p.i., with data in Figure 4A separated by day. Day 6 data are shown in Figure 4B. Two independent experiments with n = 6 (3 male, 3 female) were done and the data combined for n = 12. Bars indicate the medians, and dotted lines represent the limit of detection. No CFU were detected in feces of mock-inoculated mice. $^{**}p<0.01$, $^{***}p<0.001$, by Kruskal-Wallis test with Dunn's post-test comparing all strains.

Figure S5. The *flg*-Δ3 ON mutant elicits greater weight loss in mice. Animal weights measured every 24 hours post-inoculation expressed as a percentage of the mouse's starting weight at day 0, with data from Figure 4C separated by day; day 2 data are shown in Figure 4D. Two independent experiments with n = 6 (3 male, 3 female) were done and the data combined for n = 12. Symbols represent values from individual animals, and bars indicate the means and standard error. *p<0.05, **p<0.01, ***p<0.001 by one-way ANOVA with Tukey's post-test comparing all strains.

References

1. van der Woude MW, Baumler AJ. Phase and antigenic variation in bacteria. *Clin Microbiol Rev.* 2004;17(3):581-611.

2. Phillips ZN, Tram G, Seib KL, Atack JM. Phase-variable bacterial loci: how bacteria gamble to maximise fitness in changing environments. *Biochem Soc Trans.* Aug 30 2019;47(4):1131-1141.

3. Reyes Ruiz LM, Williams CL, Tamayo R. Enhancing bacterial survival through phenotypic heterogeneity. *PLoS Pathog.* May 2020;16(5):e1008439.

4. Cotter PA, Miller JF. BvgAS-mediated signal transduction: analysis of phase-locked regulatory mutants of *Bordetella bronchiseptica* in a rabbit model. *Infect Immun.* Aug 1994;62(8):3381-3390.

5. Weiser JN, Austrian R, Sreenivasan PK, Masure HR. Phase variation in pneumococcal opacity: relationship between colonial morphology and nasopharyngeal colonization. *Infect Immun.* Jun 1994;62(6):2582-2589.

6. Cundell DR, Weiser JN, Shen J, Young A, Tuomanen EI. Relationship between colonial morphology and adherence of *Streptococcus pneumoniae*. *Infect Immun.* Mar 1995;63(3):757-761.

7. Kim JO, Weiser JN. Association of intrastrain phase variation in quantity of capsular polysaccharide and teichoic acid with the virulence of *Streptococcus pneumoniae*. *J Infect Dis.* Feb 1998;177(2):368-377.

8. Melvin JA, Scheller EV, Miller JF, Cotter PA. *Bordetella pertussis* pathogenesis: current and future challenges. *Nat Rev Microbiol.* Apr 2014;12(4):274-288.

9. Tipton KA, Dimitrova D, Rather PN. Phase-Variable Control of Multiple Phenotypes in *Acinetobacter baumannii* Strain AB5075. *J Bacteriol.* Aug 1 2015;197(15):2593-2599.

10. Chin CY, Tipton KA, Farokhyfar M, Burd EM, Weiss DS, Rather PN. A high-frequency phenotypic switch links bacterial virulence and environmental survival in *Acinetobacter baumannii*. *Nat Microbiol.* May 2018;3(5):563-569.

11. Anderson SE, Chin CY, Weiss DS, Rather PN. Copy Number of an Integron-Encoded Antibiotic Resistance Locus Regulates a Virulence and Opacity Switch in *Acinetobacter baumannii* AB5075. *mBio.* Oct 6 2020;11(5).

12. Coyne MJ, Weinacht KG, Krinos CM, Comstock LE. Mpi recombinase globally modulates the surface architecture of a human commensal bacterium. *Proc Natl Acad Sci USA.* 2003;100(18):10446-10451.

13. Gunther NWt, Snyder JA, Lockatell V, Blomfield I, Johnson DE, Mobley HL. Assessment of virulence of uropathogenic *Escherichia coli* type 1 fimbrial mutants in which the invertible element is phase-locked on or off. *Infect Immun.* Jul 2002;70(7):3344-3354.

14. Snyder JA, Lloyd AL, Lockatell CV, Johnson DE, Mobley HL. Role of phase variation of type 1 fimbriae in a uropathogenic *Escherichia coli* cystitis isolate during urinary tract infection. *Infect Immun.* 2006;74(2):1387-1393.

15. Just I, Selzer J, Wilm M, von Eichel-Streiber C, Mann M, Aktories K. Glucosylation of Rho proteins by *Clostridium difficile* toxin B. *Nature.* Jun 8 1995;375(6531):500-503.

16. Just I, Wilm M, Selzer J, et al. The enterotoxin from Clostridium difficile (ToxA) monoglucosylates the Rho proteins. *J Biol Chem.* Jun 9 1995;270(23):13932-13936.

17. Chandrasekaran R, Lacy DB. The role of toxins in *Clostridium difficile* infection. *FEMS Microbiol Rev.* Nov 1 2017;41(6):723-750.

18. Shen A. *Clostridium difficile* toxins: mediators of inflammation. *J Innate Immun.* 2012;4(2):149-158.

19. Lyras D, O'Connor JR, Howarth PM, et al. Toxin B is essential for virulence of *Clostridium difficile*. *Nature.* 2009;458(7242):1176-1179.

20. Kuehne SA, Cartman ST, Heap JT, Kelly ML, Cockayne A, Minton NP. The role of toxin A and toxin B in *Clostridium difficile* infection. *Nature.* 2010;467(7316):711-713.

21. Carter GP, Chakravorty A, Pham Nguyen TA, et al. Defining the Roles of TcdA and TcdB in Localized Gastrointestinal Disease, Systemic Organ Damage, and the Host Response during *Clostridium difficile* Infections. *mBio.* 2015;6(3):e00551-00515.

22. Emerson JE, Reynolds CB, Fagan RP, Shaw HA, Goulding D, Fairweather NF. A novel genetic switch controls phase variable expression of CwpV, a *Clostridium difficile* cell wall protein. *Mol Microbiol.* 2009;74(3):541-556.

23. Anjuwon-Foster BR, Tamayo R. A genetic switch controls the production of flagella and toxins in *Clostridium difficile*. *PLoS Genet.* Mar 2017;13(3):e1006701.

24. Sekulovic O, Mathias Garrett E, Bourgeois J, Tamayo R, Shen A, Camilli A. Genome-wide detection of conservative site-specific recombination in bacteria. *PLoS Genet.* Apr 2018;14(4):e1007332.

25. Anjuwon-Foster BR, Maldonado-Vazquez N, Tamayo R. Characterization of flagellar and toxin phase variation in *Clostridiodes difficile* ribotype 012 isolates. *J Bacteriol.* May 7 2018;200(4): e00056-00018.

26. Garrett EM, Sekulovic O, Wetzel D, et al. Phase variation of a signal transduction system controls *Clostridioides difficile* colony morphology, motility, and virulence. *PloS Biol.* Oct 2019;17(10): e3000379.

27. Grindley NDF, Whiteson KL, Rice PA. Mechanisms of site-specific recombination. *Ann Rev Biochem.* 2006;75:567-605.

28. Johnson RC. Site-specific DNA Inversion by Serine Recombinases. *Microbiol Spectr.* 2015;3(1):MDNA3-0047-2014.

29. Sekulovic O, Bourgeois J, Shen A, Camilli A. Expanding the repertoire of conservative site-specific recombination in *Clostridioides difficile*. *Anaerobe.* Dec 2019;60:102073.

30. Reynolds CB, Emerson JE, de la Riva L, Fagan RP, Fairweather NF. The *Clostridium difficile* cell wall protein CwpV is antigenically variable between strains, but exhibits conserved aggregation-promoting function. *PLoS Pathog.* 2011;7(4):e1002024.

31. Anjuwon-Foster BR, Tamayo R. Phase variation of *Clostridium difficile* virulence factors. *Gut Microbes.* Jan 2 2018;9(1):76-83.

32. Aubry A, Hussack G, Chen W, et al. Modulation of toxin production by the flagellar regulon in *Clostridium difficile*. *Infect Immun.* 2012;80(10):3521-3532.

33. Baban ST, Kuehne SA, Barketi-Klai A, et al. The role of flagella in *Clostridium difficile* pathogenesis: comparison between a non-epidemic and an epidemic strain. *PloS One.* 2013;8(9):e73026.

34. Faulds-Pain A, Twine SM, Vinogradov E, et al. The post-translational modification of the *Clostridium difficile* flagellin affects motility, cell surface properties and virulence. *Mol Microbiol.* 2014;94(2):272-289.

35. Stevenson E, Minton NP, Kuehne SA. The role of flagella in *Clostridium difficile* pathogenicity. *Trends Microbiol.* 2015;23(5):275-282.

36. Stabler RA, He M, Dawson L, et al. Comparative genome and phenotypic analysis of *Clostridium difficile* 027 strains provides insight into the evolution of a hypervirulent bacterium. *Genome Biol.* 2009;10(9):R102.

37. Purcell EB, McKee RW, McBride SM, Waters CM, Tamayo R. Cyclic diguanylate inversely regulates motility and aggregation in *Clostridium difficile*. *J Bacteriol.* 2012;194(13):3307-3316.

38. McKee RW, Mangalea MR, Purcell EB, Borchardt EK, Tamayo R. The second messenger cyclic di-GMP regulates *Clostridium difficile* toxin production by controlling expression of *sigD*. *J Bacteriol.* 2013;195(22):5174-5185.

39. El Meouche I, Peltier J, Monot M, et al. Characterization of the SigD regulon of *C. difficile* and its positive control of toxin production through the regulation of tcdR. *PloS One.* 2013;8(12):e83748.

40. Mani N, Dupuy B. Regulation of toxin synthesis in *Clostridium difficile* by an alternative RNA polymerase sigma factor. *Proc Natl Acad Sci USA.* 2001;98(10):5844-5849.

41. Trzilova D, Anjuwon-Foster BR, Rivera DT, Tamayo R. Rho factor mediates flagellum and toxin phase variation and impacts virulence in *Clostridioides difficile*. *Plos Pathog.* Aug 2020;16(8):e1008708.

42. Trzilova D, Tamayo R. Site-Specific Recombination - How Simple DNA Inversions Produce Complex Phenotypic Heterogeneity in Bacterial Populations. *Trends Genet.* Jan 2021;37(1):59-72.

43. Gally DL, Leathart J, Blomfield IC. Interaction of FimB and FimE with the *fim* switch that controls the phase variation of type 1 fimbriae in *Escherichia coli* K-12. *Mol Microbiol.* 1996;21(4):725-738.

44. Kuehne SA, Collery MM, Kelly ML, Cartman ST, Cockayne A, Minton NP. Importance of toxin A, toxin B, and CDT in virulence of an epidemic *Clostridium difficile* strain. *J Infect Dis.* Jan 1 2014;209(1):83-86.

45. Winston JA, Thanissery R, Montgomery SA, Theriot CM. Cefoperazone-treated Mouse Model of Clinically-relevant *Clostridium difficile* Strain R20291. *J Vis Exp.* Dec 10 2016(118).

46. Chen X, Katchar K, Goldsmith JD, et al. A mouse model of *Clostridium difficile*-associated disease. *Gastroenterol.* 2008;135(6):1984-1992.

47. Warny M, Pepin J, Fang A, et al. Toxin production by an emerging strain of *Clostridium difficile* associated with outbreaks of severe disease in North America and Europe. *Lancet.* 2005;366(9491):1079-1084.

48. Dingle TC, Mulvey GL, Armstrong GD. Mutagenic analysis of the *Clostridium difficile* flagellar proteins, FliC and FliD, and their contribution to virulence in hamsters. *Infect Immun.* 2011;79(10):4061-4067.

49. Saujet L, Monot M, Dupuy B, Soutourina O, Martin-Verstraete I. The key sigma factor of transition phase, SigH, controls sporulation, metabolism, and virulence factor expression in *Clostridium difficile*. *J Bacteriol.* 2011;193(13):3186-3196.

50. Deakin LJ, Clare S, Fagan RP, et al. The *Clostridium difficile spo0A* Gene Is a Persistence and Transmission Factor. *Infect Immun.* 2012;80(8):2704-2711.

51. Pettit LJ, Browne HP, Yu L, et al. Functional genomics reveals that *Clostridium difficile* Spo0A coordinates sporulation, virulence and metabolism. *BMC Genom.* 2014;15:160-2164-2115-2160.

52. Edwards AN, Tamayo R, McBride SM. A novel regulator controls *Clostridium difficile* sporulation, motility and toxin production. *Mol Microbiol.* Jun 2016;100(6):954-971.

53. Girinathan BP, Ou J, Dupuy B, Govind R. Pleiotropic roles of *Clostridium difficile sin* locus. *PLoS Pathog.* Mar 2018;14(3):e1006940.

54. Yoshino Y, Kitazawa T, Ikeda M, et al. *Clostridium difficile* flagellin stimulates toll-like receptor 5, and toxin B promotes flagellin-induced chemokine production via TLR5. *Life Sci.* 2012;92(3):211-217.

55. Batah J, Deneve-Larrazet C, Jolivot PA, et al. *Clostridium difficile* flagella predominantly activate TLR5-linked NF-kappaB pathway in epithelial cells. *Anaerobe.* Apr 2016;38:116-124.

56. Batah J, Kobeissy H, Bui Pham PT, et al. *Clostridium difficile* flagella induce a pro-inflammatory response in intestinal epithelium of mice in cooperation with toxins. *Sci Rep.* Jun 12 2017;7(1):3256.

57. Crobach MJ, Planche T, Eckert C, et al. European Society of Clinical Microbiology and Infectious Diseases: update of the diagnostic guidance document for *Clostridium difficile* infection. *Clin Microbiol Infect.* Aug 2016;22 Suppl 4:S63-81.

58. Peltier J, Hamiot A, Garneau JR, et al. Type I toxin-antitoxin systems contribute to the maintenance of mobile genetic elements in *Clostridioides difficile*. *Commun Biol.* Nov 27 2020;3(1):718.

59. Kirk JA, Fagan RP. Heat shock increases conjugation efficiency in *Clostridium difficile*. *Anaerobe.* Dec 2016;42:1-5.

60. Bouillaut L, McBride SM, Sorg JA. Genetic Manipulation of *Clostridium difficile*. *Curr Protoc Microbiol.* 2011;Unit 9A.2:1-17.

61. Purcell EB, McKee RW, Courson DS, et al. A nutrient-regulated cyclic diguanylate phosphodiesterase controls *Clostridium difficile* biofilm and toxin production during stationary phase. *Infect Immun.* 2017;85(9):pii: e00347-00317.

62. Putnam EE, Nock AM, Lawley TD, Shen A. SpoIVA and SipL are *Clostridium difficile* spore morphogenetic proteins. *J Bacteriol.* 2013;195(6):1214-1225.

63. Edwards AN, McBride SM. Isolating and Purifying *Clostridium difficile* Spores. *Methods Mol Biol.* 2016;1476:117-128.

64. Edwards AN, McBride SM. Determination of the in vitro Sporulation Frequency of *Clostridium difficile*. *Bio Protoc.* Feb 5 2017;7(3).

905 **65.** Shrestha R, Sorg JA. Hierarchical recognition of amino acid co-germinants during
906 *Clostridioides difficile* spore germination. *Anaerobe.* Feb 2018;49:41-47.
907 **66.** George WL, Sutter VL, Citron D, Finegold SM. Selective and differential medium for
908 isolation of *Clostridium difficile*. *J Clin Microbiol.* Feb 1979;9(2):214-219.
909 **67.** Wilson KH, Kennedy MJ, Fekety FR. Use of sodium taurocholate to enhance spore
910 recovery on a medium selective for *Clostridium difficile*. *J Clin Microbiol.* Mar
911 1982;15(3):443-446.
912 **68.** Oliveira PH, Ribis JW, Garrett EM, et al. Epigenomic characterization of *Clostridioides*
913 *difficile* finds a conserved DNA methyltransferase that mediates sporulation and
914 pathogenesis. *Nat Microbiol.* Jan 2020;5(1):166-+.
915 **69.** McKee RW, Aleksanyan N, Garrett EM, Tamayo R. Type IV pili promote *Clostridium*
916 *difficile* adherence and persistence in a mouse model of infection. *Infect Immun.*
917 2018;86(5):pii: e00943-00917.

918
919

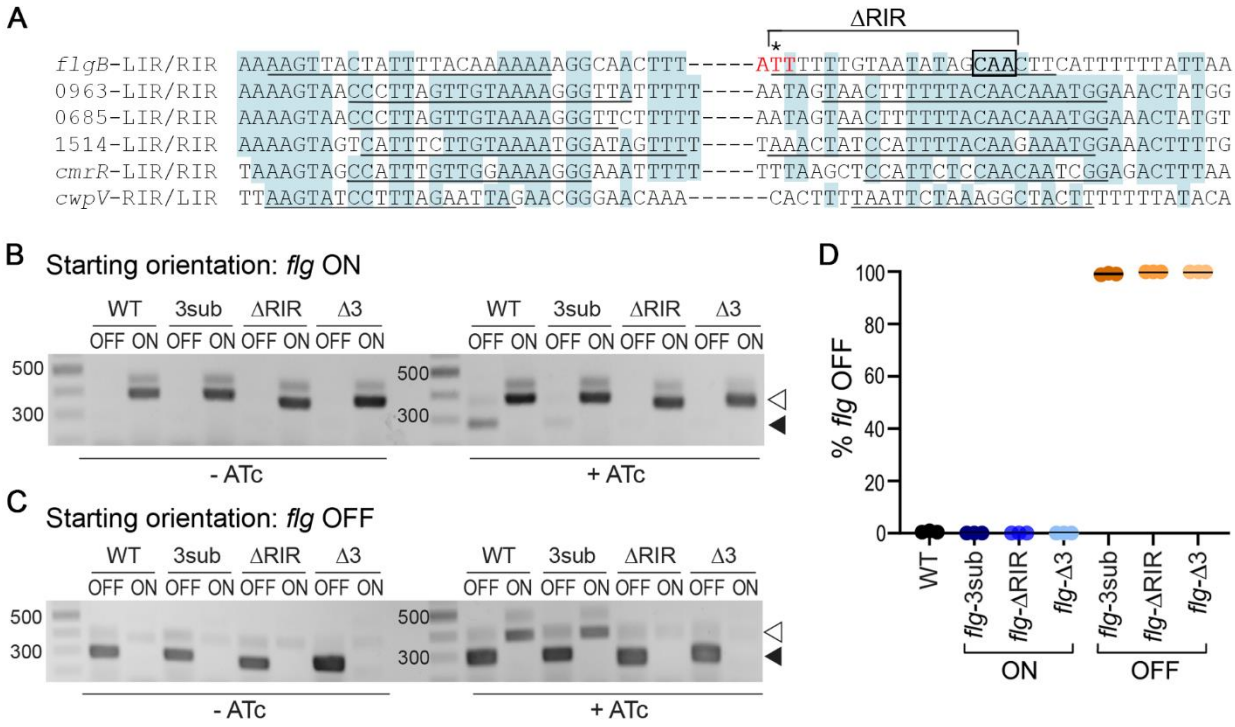

Figure 1. Mutations in *flg* RIR affect inversion in *E. coli* and *C. difficile*. A. Alignment of inverted repeats flanking the invertible DNA sequences affected by RecV. Shading denotes residues conserved in at least 4 of the 6 repeats. Putative inverted repeats are underlined. Hyphens between LIRs and RIRs represent the intervening sequences, which vary in length and nucleotide sequence. For the *flgB*-RIR, the site of cleavage by RecV is indicated with an asterisk. This nucleotide and the two adjacent residues, indicated in red, were deleted in *flg*-Δ3 constructs/strains. Note that the adenine 5' of the cleavage site is present in the *flg* ON sequence, whereas a thymine is present in *flg* OFF; constructs for mutagenesis were created in both *flg* orientations. The conserved CAA nucleotides mutated in *flg*-3sub constructs/strains are boxed in black. Nucleotides deleted in *flg*-ΔRIR bacteria/constructs are indicated. LIR, RIR = left, right inverted repeats. Numbers indicate locus tags in *C. difficile* R20291. B, C. Orientation-specific PCR to examine flagellar switch inversion in *E. coli* bearing wild-type or mutated inverted repeat target sequences. The starting orientation of the flagellar switch is indicated: *flg* ON (B) or *flg* OFF (C). Absence or presence of ATc for induction of *recV* expression is shown (-ATc/+ATc). The *flg* ON and *flg* OFF products are indicated with white and black arrows, respectively. Shown are representative images of three independent experiments. (D) Analysis of flagellar switch orientation in *C. difficile* RIR mutants by quantitative orientation-specific PCR. Means and standard deviations for three biological replicates are shown.

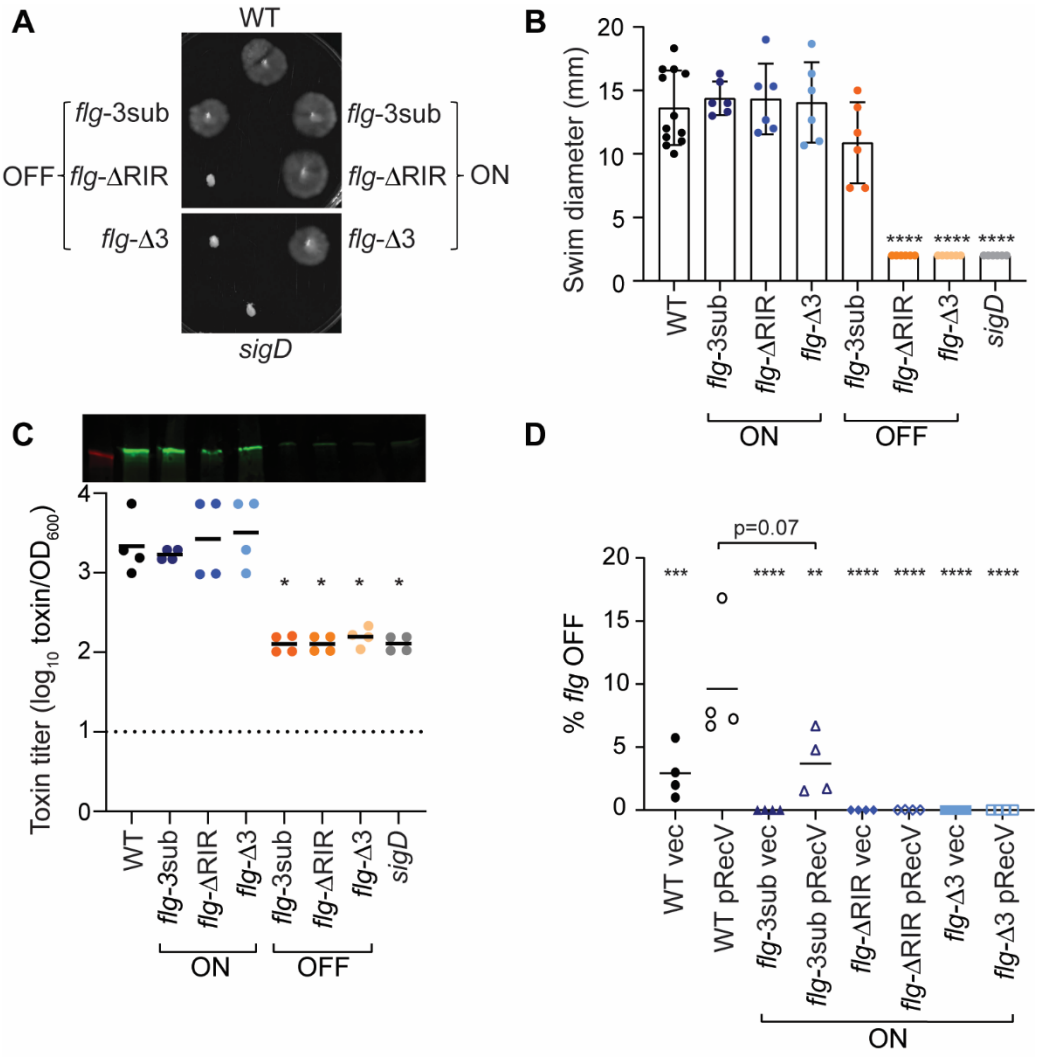

939

940 **Figure 2. Mutations in *flg* RIR affect *C. difficile* motility and toxin production.** (A)
941 Representative image of swimming motility in soft agar medium of *C. difficile* R20291 (WT),
942 *flg*-3sub ON and OFF, *flg*-ΔRIR ON and OFF, and *flg*-Δ3 ON and OFF, and *sigD*-null non-
943 motile control, incubated for 48 hours. (B) Quantification of swimming motility after 48 h of
944 strains in (A). (C) Immunoblot detection of TcdA and toxin titers after growth in TY broth. For
945 immunoblot, a representative image of three independent experiments is shown. Toxin titers of
946 supernatants from overnight bacterial cultures were calculated as the reciprocal of the highest
947 dilution that causes ≥80% rounding of Vero cells, expressed after log-transformation and
948 normalization to OD_{600} of the cultures. (B, C) Each symbol represents one biological replicate,
949 and dotted line represents the limit of detection. *p<0.05 by one-way ANOVA with Dunnett's
950 post-test comparing values to *flg*-Δ3 ON. (D) Quantitative orientation-specific PCR of the
951 flagellar switch in WT, *flg*-3sub ON, *flg*-ΔRIR ON, and *flg*-Δ3 ON mutants expressing *recV*
952 (pRecV) or bearing vector. Means and standard deviations are shown. ****p<0.0001,
953 ***p<0.001, **p<0.01 by one-way ANOVA and Dunnett's post-test comparing values to WT
954 pRecV. P value for comparison of WT pRecV and *flg*-3sub ON pRecV was determined by
955 unpaired two-tailed t-test. (B-D) Means and standard deviations are shown.

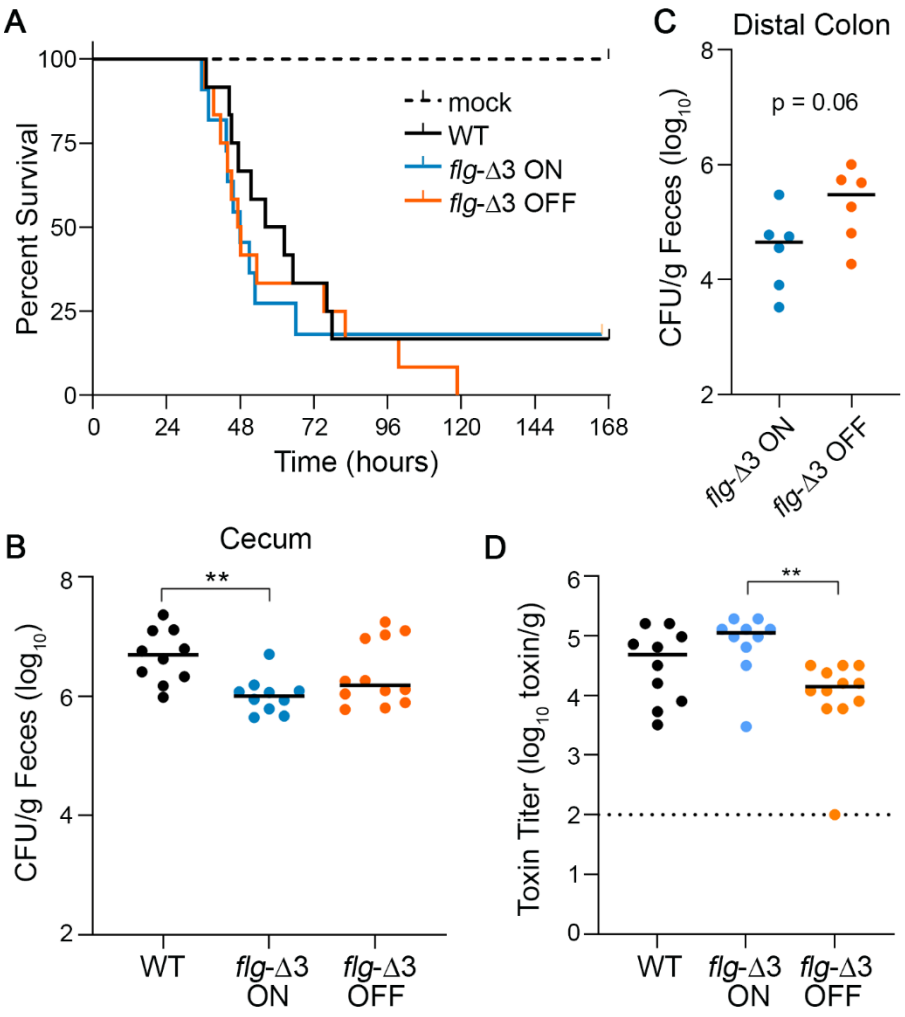

956

957 **Figure 3. Interfering with flagellar switch inversion affects toxin accumulation and**
958 **bacterial burden in a hamster model of CDI.** Antibiotic-treated male and female Syrian
959 Golden hamsters were inoculated with 1000 spores of wild-type R20291 (WT), *flg*-Δ3 ON, and
960 *flg*-Δ3 OFF. Mock-inoculated animals were included in each experiment. Data are combined
961 from two independent experiments testing strains in 3 male and 3 female hamsters, for 12 total
962 hamsters per strain. (A) Kaplan-Meier analysis of survival. (B) CFU in cecal contents. $^{**}p<0.01$
963 by Kruskal-Wallis test with Dunn's post-test. (C) CFU from homogenized distal colon from six
964 animals of one experiment. P value was determined by Mann-Whitney test. (D) Toxin titers in
965 cecal contents calculated as the reciprocal of the highest dilution to cause ≥80% rounding of
966 Vero cells. No cell rounding occurred when treated with diluted cecal contents from mock-
967 inoculated animals. Bars indicate the means; dotted line represents the limit of detection.
968 $^{**}p<0.01$ with Kruskal-Wallis test with Dunn's post-test. (B, C, D) Symbols indicate CFU from
969 individual animals and bars indicate medians.

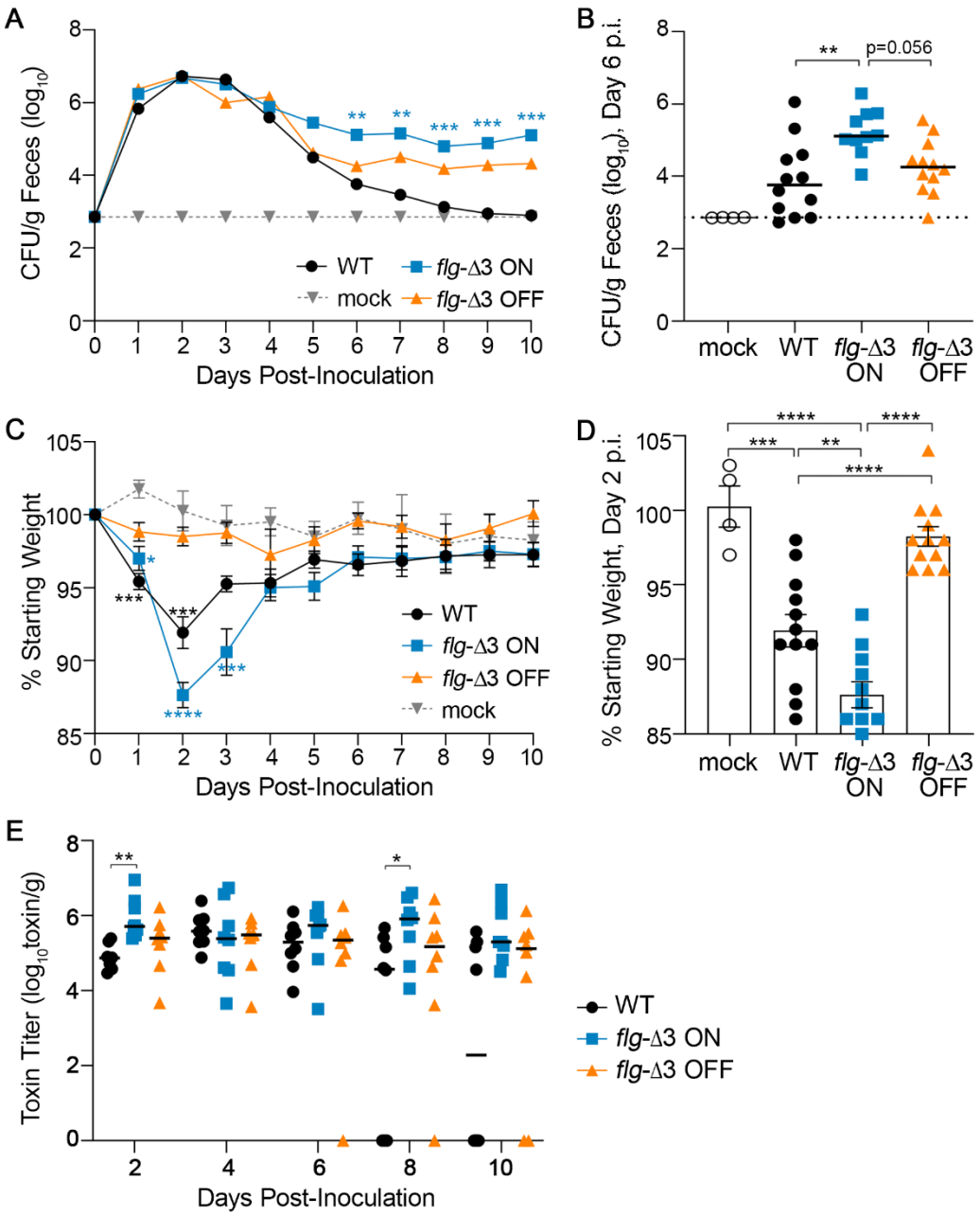

970

971 **Figure 4. Locking the flagellar switch in the ON orientation exacerbates disease and**
972 **increases persistence of *C. difficile* in a mouse model of CDI.** Antibiotic-treated male and
973 female C57BL/6 mice were inoculated with 100,000 spores of wild-type R20291 (WT), *flg*-Δ3
974 ON, and *flg*-Δ3 OFF. Mock-inoculated animals were included in each experiment. Data are
975 combined from two independent experiments testing strains in 3 male and 3 female mice, for 12
976 total mice per strain. (A) CFU enumerated in fecal samples collected every 24 hours post-
977 inoculation (p.i.). Asterisks indicate statistical comparison to WT data at that time point. (B)
978 CFU per gram feces collected on day 6 p.i.; data for days 5 - 10 shown in Figure S4. Symbols in
979 each group distinguish results from two independent experiments. (C) Animal weights

980 determined every 24 hours post-inoculation, expressed as a percentage of the mouse's weight at
981 day 0. Asterisks indicate statistical comparison to mock data at that time point. (D) Animal
982 weights at Day 2 p.i.; data for days 1 - 6 shown in Figure S5. (E) Toxin titers in fecal samples
983 calculated as the reciprocal of the highest dilution to cause ≥80% rounding of Vero cells. No cell
984 rounding occurred when treated with diluted fecal contents from mock-inoculated animals. (A-E)
985 Symbols indicate values from individual animals; dotted lines represent limit of detection. (A, B,
986 E) Bars indicate the medians. Statistical significance was determined using the Kruskal-Wallis
987 test and Dunn's post-test. (C, D) Bars indicate means and standard error. Statistical significance
988 was determined by one-way ANOVA with Tukey's post-test. *p<0.05, **p<0.01, ***p<0.001,
989 ****p<0.0001.